Acta Crystallographica Section F
Structural Biology and Crystallization Communications
ISSN 1744-3091

Crystallization and preliminary X-ray analysis of a marine diatom-infecting single-stranded RNA virus

Hisashi Naitow,[a]* Yoko Shirai,[b] Yuji Tomaru[b] and Keizo Nagasaki[b]

[a]RIKEN SPring-8 Center/RIKEN Harima Institute, 1-1-1 Kouto, Sayo-cho, Sayo-gun, Hyogo 679-5148, Japan, and [b]National Research Institute of Fisheries and Environment of Inland Sea, Fisheries Research Agency, 2-17-5 Maruishi, Hatsukaichi, Hiroshima 739-0452, Japan

Correspondence e-mail: naitow@spring8.or.jp

Received 17 May 2010
Accepted 11 August 2010

Crystals of a diatom-infecting virus (CtenRNAV) that diffracted to a resolution of 4.0 Å were grown in a mixture of 2-methyl-2,4-pentanediol (MPD), calcium chloride and sodium acetate. It was possible to freeze the crystals directly at liquid-nitrogen temperature as the reservoir solution, which included about 30% MPD, acted as a cryoprotectant during X-ray diffraction data collection. A data set was collected from a single frozen crystal obtained using this method. The crystals belonged to space group $P6_322$, with unit-cell parameters $a = b = 448.67$, $c = 309.76$ Å and two virus particles in the unit cell. The virus-particle orientation was determined using a rotation function and the virus-particle centre was estimated on the basis of crystallographic considerations. The packing of CtenRNAV in the crystal lattice was revealed by this preliminary crystallographic study.

1. Introduction

Viruses are now regarded as one of the major biological factors that control carbon cycling, microbial biomass and the genetic diversity of protists (including algae) in natural water environments (Brussaard, 2004; Suttle, 2005). Recent studies have suggested that diatom viruses may also play a prominent role in control of the dynamics of diatoms, which are significant primary producers in nature (Eissler *et al.*, 2009; Nagasaki, 2008; Tomaru *et al.*, 2009).

The diatom-infecting virus CtenRNAV is a single-stranded RNA (ssRNA) virus that infects the marine diatom *Chaetoceros tenuissimus* Meunier (Bacillariophyceae). Compared with other previously characterized algal viruses, CtenRNAV has an exceptionally high yield of $\sim10^{10}$ infectious units per millilitre. The virus particle is ~31 nm in diameter, with a capsid composed of three kinds of major protein (33.5, 31.5 and 30.0 kDa molecular mass). The genome is a linear positive-stranded RNA with a poly(A) tail at the 3′-end and is estimated to be 9.4 kb long excluding the poly(A) tail. It has two open reading frames: one encodes the replication-related proteins such as RNA helicase and RNA-dependent RNA polymerase and the other encodes the major structural proteins (Shirai *et al.*, 2008). Of the other ssRNA diatom viruses, *Chaetoceros socialis* f. *radians* RNA virus (CsfrRNAV) causes the lysis of *C. socialis* Lauder f. *radians* (Schütt) Proschkina-Lavrenko and *Rhizosolenia setigera* RNA virus (RsRNAV) causes the lysis of *R. setigera*. These diatom viruses are 22 and 32 nm in diameter, respectively, and encode three polypeptides. The viruses harbour genomes of about 9.4 and 11.2 kb in length without a poly(A) tail and yield 5×10^7 and 3.5×10^8 infectious units per millilitre, respectively (Tomaru *et al.*, 2009; Nagasaki *et al.*, 2004). Therefore, the typical yields of these other diatom-infecting ssRNA viruses of between 10^7 and 10^8 infectious units per millilitre are two or three orders of magnitude lower than the yield of CtenRNAV (Shirai *et al.*, 2008). The monophyly of CtenRNAV and the two other diatom-infecting ssRNA viruses CsfrRNAV and RsRNAV was strongly supported by phylogenetic analysis of the RNA-dependent RNA domain (Shirai *et al.*, 2008; Tomaru *et al.*, 2009); thus, a new genus, *Bacillarnavirus*, has recently been proposed for these diatom-infecting ssRNA viruses. Here, we report the crystallization of CtenRNAV and initial analysis of the X-ray diffraction data, which

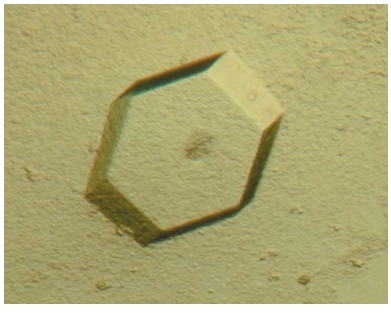

will permit the first structure-based analysis of a diatom-infecting ssRNA virus.

2. Materials and methods

2.1. Algal cultures

C. tenuissimus strain 2-10 was grown in SWM3 medium (Chen *et al.*, 1969; Itoh & Imai, 1987) enhanced with 2 n*M* Na_2SeO_3 using a 12 h light/12 h dark cycle with ∼110 µmol photons m^{-2} s^{-1} provided as cool white fluorescent lighting at 288 K.

2.2. Virus purification

A logarithmic phase culture of *C. tenuissimus* 2-10 (500 ml) was inoculated with CtenRNAV and incubated for 10 d to cause lysis. The viral lysate was sequentially passed through 0.8 and 0.2 µm polycarbonate membrane filters (Nuclepore) to eliminate cellular debris. Polyethylene glycol 6000 was added to the filtrate to a final concentration of 10%(*w*/*v*). The virus suspension was incubated overnight at 277 K in the dark. After centrifugation at 57 000*g* at 277 K for 1.5 h, the resultant pellet was suspended in 20 ml 10 m*M* phosphate buffer pH 7.2. An equal volume of chloroform was then added to the suspension. After intensive stirring, the suspension was centrifuged at 7500*g* for 20 min at 277 K. The supernatant was then centrifuged at 217 000*g* for 4 h at 277 K and the virus particles were suspended in 600 µl ultrapure water. Finally, the viral suspension was concentrated tenfold using a Microcon YM-30 (Millipore). The final concentration of the viral suspension was about 10 mg ml^{-1}.

2.3. Crystallization

Commercial crystallization screening kits (Crystal Screen and Crystal Screen 2 from Hampton Research) were employed to determine initial crystallization conditions. Crystallization experiments were carried out using the hanging-drop vapour-diffusion method. Typically, 3 µl viral suspension was added to 3 µl reservoir solution and the droplet was incubated at 293 K over 1.0 ml reservoir solution. Crystalline structures appeared under several crystallization conditions in the presence of polyethylene glycol (PEG) or 2-methyl-2,4-pentanediol (MPD; Fig. 1). These conditions were improved to obtain higher reproducibility. The best crystals were obtained using 27% MPD and 0.03 *M* $CaCl_2$ at pH 4.6 in 0.1 *M* sodium acetate after about 2 d.

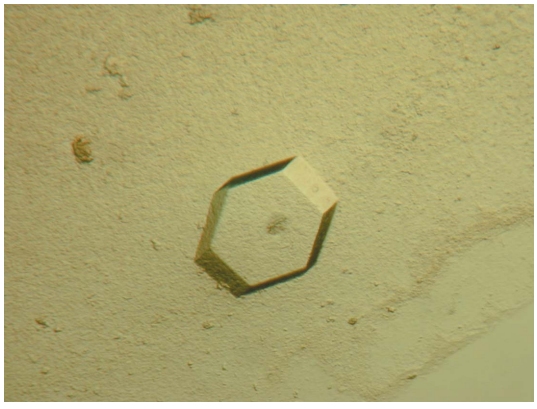

Figure 1
The first crystal of CtenRNAV obtained from 30% 2-methyl-2,4-pentanediol (MPD), 0.02 *M* calcium chloride and 0.1 *M* sodium acetate pH 4.6. The crystal dimensions are about 0.2 × 0.25 × 0.2 mm.

Table 1
Experimental conditions, crystal data and diffraction statistics.

Values in parentheses are for the outer shell.

Beamline	Spring-8 BL44B2
Detector	Rigaku Jupiter 210
No. of images	180
Oscillation width (°)	0.5
Wavelength (Å)	1.0
Crystal-to-detector distance (mm)	300
Exposure time (s)	40
Crystal lattice	Hexagonal
Unit-cell parameters (Å)	$a = b = 448.67$, $c = 309.76$
Space group	$P6_322$
Calculated V_M (Å^3 Da^{-1})	3.1
Perfect twinning test†	1.93
Total reflections	713097
Unique reflections	127675
Rejected reflections	10885
Resolution (Å)	82.29–4.00 (4.07–4.00)
R_{merge}‡	24.5 (34.4)
Multiplicity	5.6 (2.7)
Completeness (%)	82.3 (55.5)
$\langle I/\sigma(I)\rangle$	3.2 (1.6)

† The perfect twinning test calculates $\langle I^2\rangle/\langle I\rangle^2$, which has a value of 2.0 for an untwinned crystal and 1.5 for a perfectly twinned crystal. ‡ $R_{merge} = \sum_{hkl}\sum_i |I_i(hkl) - \langle I(hkl)\rangle|/\sum_{hkl}\sum_i I_i(hkl) \times 100$, where $I_i(hkl)$ is the ith observed diffraction intensity with reflection index hkl and $\langle I(hkl)\rangle$ is the averaged intensity over crystallographic symmetry-equivalent measurements.

2.4. Data collection and X-ray analysis

Crystals were directly mounted on a cryoloop from the mother liquor and immediately placed in a nitrogen-gas stream. Diffraction data collection at cryogenic temperature was carried out on BL44B2 at SPring-8. Monochromatic X-rays (λ = 1.0 Å) were used with an oscillation angle of 0.5° and an exposure time of 40 s. Diffraction images were collected using a Rigaku Jupiter 210 CCD detector at a crystal-to-detector distance of 300 mm. Diffraction data reduction was carried out with the program *HKL*-2000 (Otwinowski & Minor, 1997). A perfect twinning test was performed with the program *SFCHECK* (Vaguine *et al.*, 1999) from the *CCP*4 program suite (Collaborative Computational Project, Number 4, 1994). The value obtained for $\langle I^2\rangle/\langle I\rangle^2$ was 1.93, meaning that the CtenRNAV crystal was untwinned. The $\kappa = 72°$ section of the rotation function was calculated using diffraction data between 40 and 10 Å resolution for the observed data using the program *GLRF* (Tong & Rossmann, 1997) with a radius of integration of 150 Å.

3. Results and discussion

3.1. Data collection

The crystallization condition, which included about 30% MPD, was considered to function as a cryoprotectant. We attempted to directly freeze the CtenRNAV crystal picked up from the mother liquor in a Cryostream at liquid-nitrogen temperature. One of the frozen crystals diffracted to approximately 4.0 Å resolution and a data set was collected on BL44B2 at SPring-8.

3.2. Analysis of the X-ray diffraction data

180 diffraction images were collected from the single frozen CtenRNAV crystal. After performing data reduction with the *HKL*-2000 program, we found symmetry-related peaks with good agreement with Laue class 6/*mmm* in the rotation-function calculation. The crystal belonged to space group $P6_322$, with unit-cell parameters $a = b = 448.67$, $c = 309.76$ Å, according to the systematic absences that were detected. The processed data were 82.3% complete between

82.29 and 4.0 Å resolution, with a merging R of 24.5% on X-ray intensities. In the outer resolution shell (4.07–4.0 Å resolution), the completeness was 55.5% and the resultant merging R was 34.4% (Table 1). The CtenRNAV crystal was very fragile and cracking frequently occurred on mounting the crystal on a cryoloop. We searched for a crystallization condition that would overcome this fragility, but were unable to find a better crystallization condition. The reason for the relatively poor data quality, particularly in the outer resolution shell, was that data collection had to be performed using the fragile crystals that could be frozen without cracking. It appears that it will be necessary to perform a search for a crystallization condition using a different precipitant in order to obtain a better crystal. The average mosaic spread of the CtenRNAV crystal was 0.288°. Assuming the presence of two virus particles in the unit cell, $V_{\rm M}$ was 3.1 Å^3 Da^{-1} and the solvent content $V_{\rm solv}$ was 0.60 [$V_{\rm solv} = 1 - (1.23/V_{\rm M})$], assuming that the molecular mass of one virus particle is 9924 kDa (the capsid has a mass of 5700 kDa and the two ssRNA molecules have a mass of 4224 kDa). This solvent content strongly supports the hypothesis that two virus particles are present in the unit cell (Matthews, 1968). Fig. 2 shows a self-rotation function ($\kappa = 72^\circ$ section) that indicates the fivefold symmetry axes of the two virus particles in the unit cell. It consists of groups of peaks derived from two virus particles 1 and 2. All of the major peaks in the $\kappa = 72^\circ$ section coincided with forecasted icosahedral fivefold positions for each particle orientation (Figs. 3*a* and 3*b*). These orientations indicate that the icosahedral twofold and threefold axes of the virus particles are parallel to the corresponding crystallographic symmetry axes. The two virus-particle centres estimated by packing considerations in space group $P6_322$ were located on a 32 point-group symmetry operator in a special position with Wyckoff notation *c* or *d* (*International Tables for X-ray Crystallography*, 1969). We calculated the structure factors at low resolution (45 Å) by using the backbone

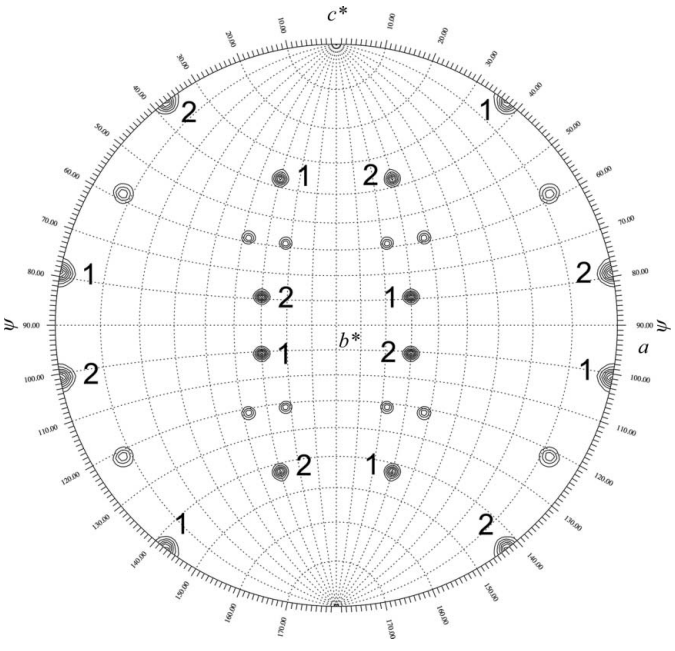

Figure 2
A stereographic projection of the $\kappa = 72^\circ$ section of the CtenRNAV self-rotation function calculated using the diffraction data. The observed data in the resolution range 40–10 Å were used in the computation, with a radius of integration of 150 Å. Peaks labelled '1' are for particle 1 in Table 2 and peaks labelled '2' are for particle 2. Unlabelled (minor) peaks are assumed to result from cross-peaks between particles 1 and 2.

Table 2
Virus-particle orientations and positions.

The meaning of the virus-particle orientation (φ, ψ, κ) is identical to that used by the *CCP*4 program suite. (x, y, z) are deorthogonalized fractional coordinates.

Particle	φ (°)	ψ (°)	κ (°)	x	y	z
1	165.0	69.5	285.5	2/3	1/3	3/4
2	165.0	110.5	74.5	1/3	2/3	1/4

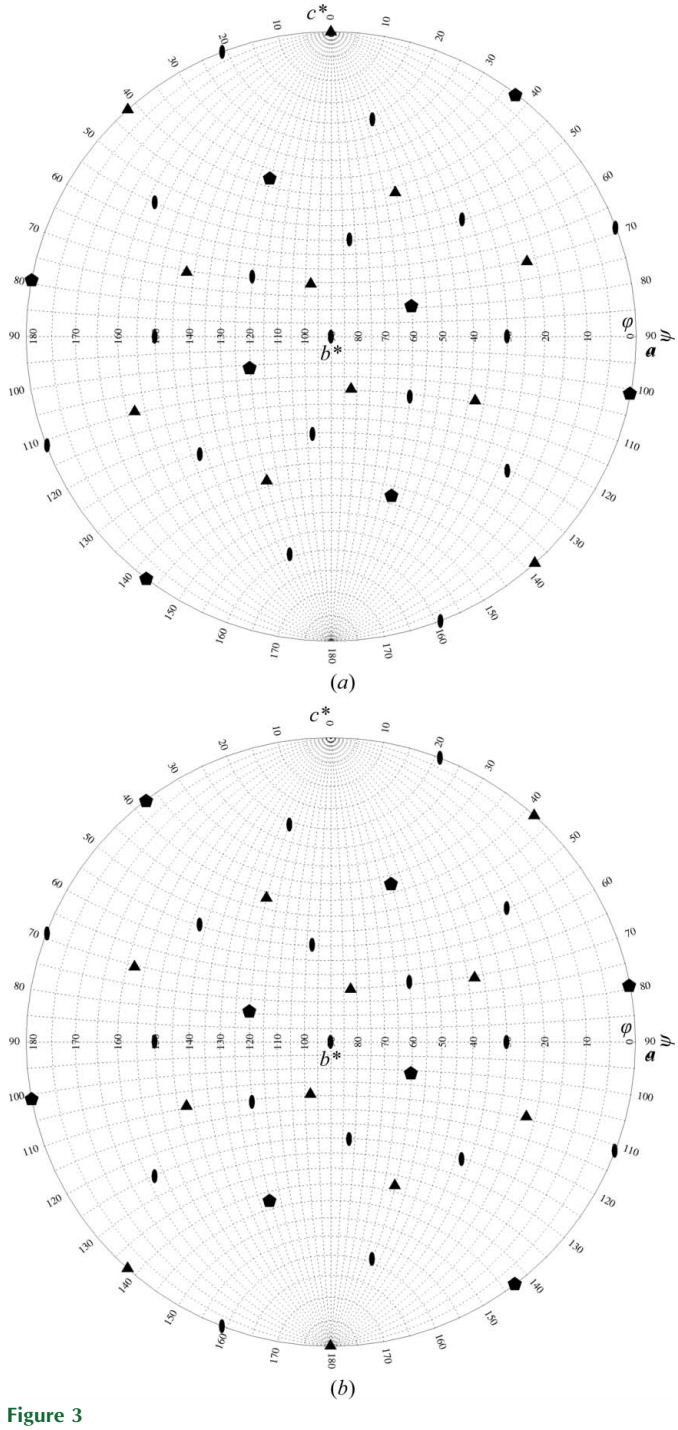

Figure 3
Stereographic projections describing the orientations of icosahedral twofold, threefold and fivefold axes for (*a*) particle 1 and (*b*) particle 2. In each particle, one of the icosahedral twofold axes is parallel to the crystallographic *b* axis and one of the icosahedral threefold axes is parallel to the crystallographic *c* axis. The quantitative notations for the orientation (φ, ψ, κ) of each particle are shown in Table 2.

atoms of cricket paralysis virus (Tate *et al.*, 1999) as an examination model in order to test the two potential solutions. The *R* factors of the structure factors against the observed diffraction data to 45 Å resolution were 0.55 and 0.58, respectively. This indicates that Wyckoff notation *c* is correct. The resultant virus-particle orientations and positions are shown in Table 2.

We have revealed the virus-particle orientations and positions in the crystal lattice. Therefore, calculation of the initial phasing model could be used for structure determination using real-space averaging and phase extension carried out according to the viral orientation and position. The crystallization conditions will require significant improvement for structure determination at atomic resolution.

This research was partially supported by a grant from the Ministry of Education, Culture, Sports, Science and Technology (MEXT) of Japan to HN and a Grant-in-Aid for Scientific Research (A) (No. 20247002) from the Ministry of Education, Culture, Sports, Science and Technology (MEXT) of Japan to KN and YT. HN acknowledges support from Dr T. Ishikawa (RIKEN SPring-8 Center).

References

Brussaard, C. P. (2004). *J. Eukaryot. Microbiol.* **51**, 125–138.
Chen, L. C.-M., Edelstein, T. & McLachlan, J. (1969). *J. Phycol.* **5**, 211–220.
Collaborative Computational Project, Number 4 (1994). *Acta Cryst.* D**50**, 760–763.
Eissler, Y., Wang, K., Chen, F., Wommack, K. E. & Coats, D. W. (2009). *J. Phycol.* **45**, 787–797.
International Tables for X-ray Crystallography (1969). Vol. I, edited by N. F. M. Henry & K. Lonsdale, p. 289. Birmingham: Kynoch Press.
Itoh, K. & Imai, I. (1987). *A Guide for Studies of Red Tide Organisms*, edited by Japan Fisheries Resource Conservation Association, pp. 122–130. Tokyo: Shuwa.
Matthews, B. M. (1968). *J. Mol. Biol.* **33**, 491–497.
Nagasaki, K. (2008). *J. Microbiol.* **46**, 235–243.
Nagasaki, K., Tomaru, Y., Katanozaka, N., Shirai, Y., Nishida, K., Itakura, S. & Yamaguchi, M. (2004). *Appl. Environ. Microbiol.* **70**, 704–711.
Otwinowski, Z. & Minor, W. (1997). *Methods Enzymol.* **276**, 307–326.
Shirai, Y., Tomaru, Y., Takao, Y., Suzuki, H., Nagumo, T. & Nagasaki, K. (2008). *Appl. Environ. Microbiol.* **74**, 4022–4027.
Suttle, C. A. (2005). *Nature (London)*, **437**, 356–361.
Tate, J., Liljas, L., Scotti, P., Christian, P., Lin, T. & Johnson, J. E. (1999). *Nature Struct. Biol.* **6**, 765–774.
Tomaru, Y., Takao, Y., Suzuki, H., Nagumo, T. & Nagasaki, K. (2009). *Appl. Environ. Microbiol.* **75**, 2375–2381.
Tong, L. & Rossmann, M. G. (1997). *Methods Enzymol.* **276**, 594–611.
Vaguine, A. A., Richelle, J. & Wodak, S. J. (1999). *Acta Cryst.* D**55**, 191–205.